

Imidazolium Hexacyanidosilicates

Hexacyanidosilicates with Functionalized Imidazolium Counterions

Jörg Harloff,^[a] Karoline Charlotte Laatz,^[a] Swantje Lerch,^[c] Axel Schulz,^{*,[a,b]} Philip Stoer,^[a] Thomas Strassner,^{*,[c]} and Alexander Villinger^[a]

Abstract: Functionalized imidazolium cations were combined with the hexacyanidosilicate anion, $[\text{Si}(\text{CN})_6]^{2-}$, by salt metathesis reactions with $\text{K}_2[\text{Si}(\text{CN})_6]$, yielding novel ionic compounds of the general formula $[\text{R}-\text{Ph}(n\text{Bu})\text{Im}]_2[\text{Si}(\text{CN})_6]$ {R = 2-Me (**1**), 4-Me (**2**), 2,4,6-Me = Mes (**3**), 2-MeO (**4**), 2,4-F (**5**), 4-Br (**6**); Im = imidazolium}. All synthesized imidazolium hexacyanidosilicates decompose upon thermal treatment above 95 °C (96 – 164 °C). Furthermore, the hexa-borane-adduct $[\text{Mes}(n\text{Bu})\text{Im}]_2-$

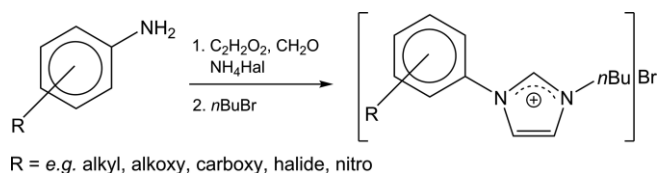
$\{\text{Si}[(\text{CN})\text{B}(\text{C}_6\text{F}_5)_3]_6\} \cdot 6\text{CH}_2\text{Cl}_2$ (**7**), which is thermally stable up to 215 °C, was obtained from the reaction of **3** with Lewis acidic $\text{B}(\text{C}_6\text{F}_5)_3$. In CH_3CN solution, decomposition of the hexaadduct to the Lewis-acid-base adduct $\text{CH}_3\text{CN}-\text{B}(\text{C}_6\text{F}_5)_3$ and $[(\text{C}_6\text{F}_5)_3\text{B}(\mu-\text{CN})-\text{B}(\text{C}_6\text{F}_5)_3]^-$ was observed. All synthesized compounds were isolated in good yields and were completely characterized including single crystal structure elucidations.

Introduction

It was Paul Walden in 1914, who synthesized $[\text{EtH}_3\text{N}]\text{NO}_3$ (m.p. 12 °C), one of the first known ionic liquids (IL).^[1] Due to weak Coulomb interactions between organic cations and organic or inorganic anions, such salts usually possess a low melting point (< 100 °C) and are also referred to as *room temperature ionic liquids* (RTILs) if the melting point is below 25 °C. By combining cations and anions in a wide variety of ways, or by selectively modifying organic groups of the ions, physical properties such as melting point, viscosity, high thermal stability, volatility and acidity can be influenced, which is why ILs are also called “designer solvents”.^[2] Due to these variable properties, ILs have been extensively investigated in recent years and have been used, for example, as solvents in organic and catalytic syntheses,^[2–5] as electrolyte liquids in batteries,^[6–9] as addi-

tives in dye cells,^[10–12] as extraction media for metals^[13–15] or for the synthesis of nanoparticles^[16,17] and metal clusters.^[18–20] Furthermore, they are used in processes such as dissolving of cellulose^[21] or for the synthesis of alkoxyphenyl-phosphines in the industrial BASIL™ process.^[22,23]

One class of cations in IL chemistry, which are often used, are imidazolium cations, as they can easily be substituted at the nitrogen atoms and / or at the C–H acidic position of the five-membered ring with linear or branched alkyl chains of different lengths.^[24] So called *tunable aryl alkyl ionic liquids* (TAAILs) allow a much greater diversity as they exhibit an aryl and an alkyl moiety at the heteroatoms of the imidazolium cation. They offer interesting electronic effects, which can be introduced at the phenyl ring system by changing type, number and position of the substituents. The TAAILs are easily accessible by a two-step synthesis protocol. First, an aniline derivative, glyoxal, formaldehyde and an ammonium halide are converted in an one-pot reaction. In a second step a nucleophilic substitution of the imidazole leads to the imidazolium halide salt (Scheme 1).^[25–27]



Scheme 1. Syntheses of Tunable Aryl Alkyl Ionic Liquids (TAAILs).

We were interested to synthesize new ionic liquids by combining the properties of the low-melting TAAILs with the hexacyanidosilicate dianion, $[\text{Si}(\text{CN})_6]^{2-}$. Just recently, we reported on the successful synthesis of the cyanido(fluorido)-silicate dianions. Via temperature controlled F^- / CN^- exchange reactions of ammonium fluoridosilicates in an excess of neat $\text{Me}_3\text{Si}-\text{CN}$,

[a] Dr. J. Harloff, K. C. Laatz, Prof. Dr. A. Schulz, P. Stoer, Dr. A. Villinger
Anorganische Chemie, Institut für Chemie, Universität Rostock
18059 Rostock, A.-Einstein-Str. 3a, Germany
E-mail: axel.schulz@uni-rostock.de
<https://www.schulz.chemie.uni-rostock.de/>

[b] Prof. Dr. A. Schulz
Materialdesign, Leibniz-Institut für Katalyse an der Universität Rostock
18059 Rostock, A.-Einstein-Str. 29a, Germany

[c] S. Lerch, Prof. Dr. T. Strassner
Physikalische Organische Chemie, Technische Universität Dresden
01069 Dresden, Bergstraße 66, Germany
E-mail: thomas.strassner@chemie.tu-dresden.de
<https://tu-dresden.de/mn/chemie/oc/oc3/die-professur/prof-dr-thomas-strassner/index>

Supporting information and ORCID(s) from the author(s) for this article are available on the WWW under <https://doi.org/10.1002/ejic.202000281>.

© 2020 The Authors. Published by Wiley-VCH Verlag GmbH & Co. KGaA. This is an open access article under the terms of the Creative Commons Attribution-NonCommercial-NoDerivs License, which permits use and distribution in any medium, provided the original work is properly cited, the use is non-commercial and no modifications or adaptations are made.

we were able to form salts with $[\text{SiF}(\text{CN})_5]^{2-}$ and $[\text{Si}(\text{CN})_6]^{2-}$ as counter anions. A facile neutralization reaction in water of KOH with protic ammonium salts, such as $[\text{nPr}_3\text{NH}]_2[\text{Si}(\text{CN})_6]$, enabled access to amorphous, solvent free potassium hexacyanidosilicate after drying in vacuo. Crystallization at low temperatures from a concentrated acetonitrile solution led to formation of $\text{K}_2[\text{Si}(\text{CN})_6] \cdot 6\text{CH}_3\text{CN}$. In a subsequent salt metathesis of the solvent free $\text{K}_2[\text{Si}(\text{CN})_6]$ with $[\text{BMIm}]\text{Br}$ ($\text{BMIm} = 3\text{-Butyl-1-methylimidazolium}$), the ionic liquid $[\text{BMIm}]_2[\text{Si}(\text{CN})_6]$ ($T_{\text{m.p.}} 72^\circ\text{C}$) was obtained.^[28]

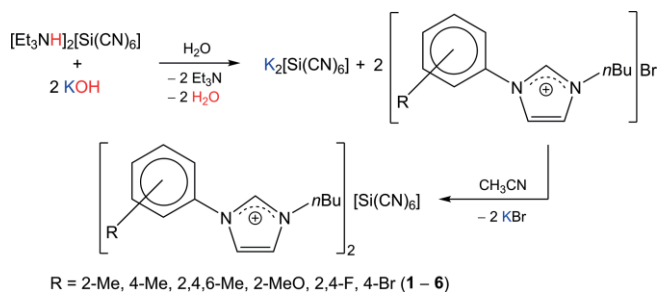
Simultaneously to our publication, Portius and co-workers reported on a further synthesis strategy for the preparation of $[\text{PPN}]_2[\text{Si}(\text{CN})_6]$ ($[\text{PPN}]^+ = \text{Bis}(\text{triphenylphosphine})\text{iminium}$) as well as on the heavier homologues of germanium and tin ($[\text{PPN}]_2[\text{Ge}(\text{CN})_6]$ and $[\text{PPN}]_2[\text{Sn}(\text{CN})_6]$).^[29]

Here we report on the solvent free structure of $\text{K}_2[\text{Si}(\text{CN})_6]$ and on the synthesis of different substituted phenyl-*n*-butylimidazolium hexacyanidosilicate salts. None of these salts can be classified as IL, since only decomposition of the compounds was observed at elevated temperatures. Furthermore, we examined the reaction of $[\text{Mes}(\text{nBu})\text{Im}]_2[\text{Si}(\text{CN})_6]$ towards the Lewis acid $\text{B}(\text{C}_6\text{F}_5)_3$ that led to the formation of a very bulky hexa-adduct.

Results and Discussion

Synthesis and Properties of $[\text{R-Ph}(\text{nBu})\text{Im}]_2[\text{Si}(\text{CN})_6]$ ($\text{R} = 2\text{-Me}$ (**1**), 4-Me (**2**), $2,4,6\text{-Me} = \text{Mes}$ (**3**), 2-MeO (**4**), $2,4\text{-F}$ (**5**), 4-Br (**6**)) and $[\text{Mes}(\text{nBu})\text{Im}]_2[\text{Si}(\text{CN})_6 \cdot \text{B}(\text{C}_6\text{F}_5)_3]_6 \cdot 6 \text{CH}_2\text{Cl}_2$ (**7**))

We started this project with the synthesis of $\text{K}_2[\text{Si}(\text{CN})_6]$ by treating $[\text{Et}_3\text{NH}]_2[\text{Si}(\text{CN})_6]$ with two equivalents of KOH in water (Scheme 2), according to a slightly changed literature known process mentioned above.^[28] The potassium salt was isolated by fractional crystallization from the mother lye. Single crystals could be obtained, suitable for X-ray analysis (Figure 1) which revealed the formation of a solvent-free structure. According to EA, the water content amounts to approx. 1.4 wt.-% $\{\text{K}_2[\text{Si}(\text{CN})_6] \cdot 0.2\text{H}_2\text{O}\}$. All following imidazolium hexacyanidosilicates, generalized as $[\text{R-Ph}(\text{nBu})\text{Im}]_2[\text{Si}(\text{CN})_6]$ ($\text{R} = 2\text{-Me}$ (**1**), 4-Me (**2**), $2,4,6\text{-Me} = \text{Mes}$ (**3**), 2-MeO (**4**), $2,4\text{-F}$ (**5**), 4-Br (**6**)) were prepared by facile salt metathesis reactions of $\text{K}_2[\text{Si}(\text{CN})_6]$ with two equivalents of $[\text{R-Ph}(\text{nBu})\text{Im}]\text{Br}$ in acetonitrile (Scheme 2). The compounds were purified by filtering off KBr and isolated



Scheme 2. Synthesis of $\text{K}_2[\text{Si}(\text{CN})_6]$ and subsequent formation of imidazolium hexacyanidosilicates by salt metathesis reactions in acetonitrile.

by crystallization (specifications in experimental details). Since all obtained imidazolium salts tend to decompose at elevated temperatures without melting, none of these salts can be regarded as IL. Yields and decomposition points are listed in Table 1.

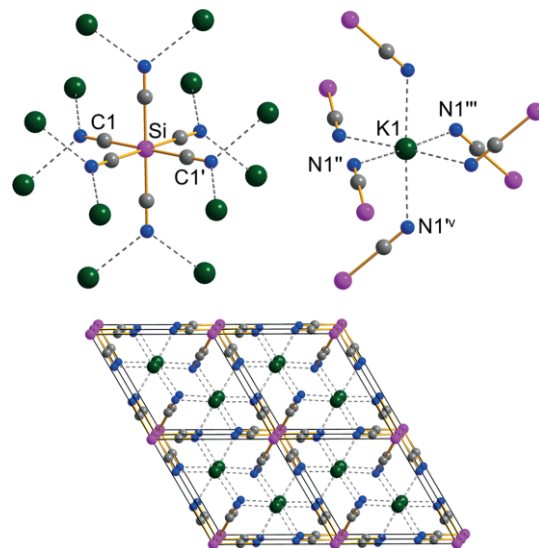


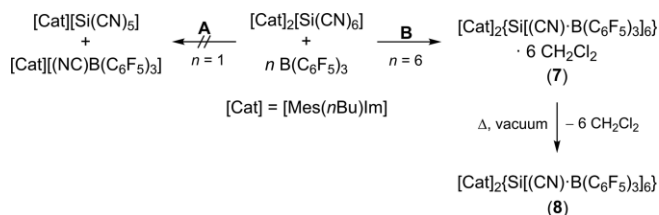
Figure 1. Ball-and-stick representation of the octahedral environment of $[\text{Si}(\text{CN})_6]^{2-}$ (top left), K^+ (top right) of the molecular ions in the crystal structure of $\text{K}_2[\text{Si}(\text{CN})_6]$. Bottom: view along *c*-axis of a $2 \times 2 \times 2$ cells representation of the 3D network. Selected bond lengths [Å] and angles [°]: Si–C1 1.9506(8), N1^{II}–K1 2.836(1); C1–Si1–C1^I 180.0, N1^{II}–K1–N1^{III} 177.57(3), N1^{II}–K1–N1^{IV} 87.05(3). Symmetry code: (I) $-x + y, -x, 1 - z$; (II) $x, x - y, 2 - z$; (III) $-x + y, -x, 1 + z$; (IV) $x, -1 + y, 1 + z$.

Table 1. Decomposition temperatures [$^\circ\text{C}$] (heating rate 5 K min^{-1}) and yields [%] of all synthesized compounds.

# (R)	$T_{\text{dec.}}$	yield	# (R)	$T_{\text{dec.}}$	yield
1 (2-Me)	164	67	5 (F)	96	43
2 (4-Me)	119	55	6 (Br)	138	69
3 (Mes)	146	54	7	215	/
4 (2-MeO)	125	55	8	230	80

Besides the synthesis of imidazolium hexacyanidosilicates, we were also interested in studying the reactivity of the hexacyanidosilicate anion towards strong Lewis acids such as $\text{B}(\text{C}_6\text{F}_5)_3$. This Lewis-acid-base reaction was hampered in the past, since ammonium hexacyanidosilicate salts were only soluble in polar solvents such as acetonitrile, which itself forms a Lewis-acid-base adduct with the borane.^[30] Therefore, $[\text{Mes}(\text{nBu})\text{Im}]_2[\text{Si}(\text{CN})_6]$ was chosen as starting material because the cation allows the salt to dissolve in non-Lewis basic solvents such as dichloromethane. Initially, we aimed to synthesize pentavalent $[\text{Si}(\text{CN})_5]^-$ salts by abstracting a cyanide moiety with $\text{B}(\text{C}_6\text{F}_5)_3$ (Scheme 3, route **A**). Thus, one equivalent of $\text{B}(\text{C}_6\text{F}_5)_3$ and $[\text{Mes}(\text{nBu})\text{Im}]_2[\text{Si}(\text{CN})_6]$ were dissolved in dichloromethane. However, only different substitution patterns of silicate-borane adducts and remaining hexacyanidosilicate were observed by means of $^{13}\text{C}\{^1\text{H}\}$ and $^{19}\text{F}\{^1\text{H}\}$ NMR experiments but no product species could be isolated from the mixture. Hence, the procedure was repeated but with an excess ($n = 6$) of $\text{B}(\text{C}_6\text{F}_5)_3$

(Scheme 3, route **B**). The starting materials were dissolved in dichloromethane and both solutions were combined afterwards. The mixture was immediately placed at a non-vibrating location which led to the formation of small crystals of $[\text{Mes}(n\text{Bu})\text{Im}]_2\{\text{Si}[(\text{CN})\cdot\text{B}(\text{C}_6\text{F}_5)_3]_6\}\cdot 6\text{CH}_2\text{Cl}_2$ (**7**) within several minutes in good yields (see Table 1).



Scheme 3. Reaction of **3** with different equivalents of $\text{B}(\text{C}_6\text{F}_5)_3$ ($n = 1$ or 6). Route **A**: Assumed synthesis of $[\text{Si}(\text{CN})_5]^-$ and $[(\text{NC})\text{B}(\text{C}_6\text{F}_5)_3]^-$ containing salts ($n = 1$). Route **B**: Complete hexa-substitution of $[\text{Si}(\text{CN})_6]^{2-}$ by $\text{B}(\text{C}_6\text{F}_5)_3$ ($n = 6$) forming the $[\text{Si}[(\text{CN})\cdot\text{B}(\text{C}_6\text{F}_5)_3]_6]^{2-}$ anion as CH_2Cl_2 solvate (**7**) which can be transferred to the solvent-free form **8** upon drying at elevated temperatures.

Crystals of **7** were investigated by X-ray (Figure 4) and thermogravimetric analysis (TGA). The compound decomposes at elevated temperature ($T_{\text{dec.}} = 215$ °C) and due to TGA experiments, loss of co-crystallized CH_2Cl_2 was observed (Heating rate 5 K min^{-1} , ESI Figure S41). The solvent-free form **8** ($T_{\text{dec.}} = 230$ °C) was obtained when **7** was gently dried at 100 °C under reduced pressure as proven by EA. Furthermore, the salt was characterized in solution by means of NMR experiments. Since **8** is only sparingly soluble in $[\text{D}_2]$ dichloromethane, no $^{13}\text{C}\{^1\text{H}\}$ / $^{29}\text{Si}\{\text{IG}\}$ NMR signals for the $[\text{Si}(\text{CN})_6]$ core were observed. The $^{11}\text{B}\{^1\text{H}\}$ NMR resonance for the coordinating $\text{B}(\text{C}_6\text{F}_5)_3$ moieties was found at -9.9 ppm with a large line width of $\Delta\nu_{1/2} = 1060$ Hz. A broad signal shape is a well-known phenomenon for compounds in which the $\text{B}(\text{C}_6\text{F}_5)_3$ moieties coordinate to the nitrogen of the nitriles.^[31–33] The effect of broadening might be further enhanced due to a slowed rotational reorientation due to the significant size of the anion. With respect to uncoordinated, naked $\text{B}(\text{C}_6\text{F}_5)_3$ (59.1 ppm in CD_2Cl_2),^[34] this signal is considerably shifted to lower frequencies but found in the expected region as reported for other 4-coordinated cyanidoborates (Table 2).^[34]

Table 2. Selected bond lengths [Å], $^{11}\text{B}\{^1\text{H}\}$ NMR [ppm] and Raman [cm^{-1}] spectroscopic data of **3** and **7** along with reference materials [dca_2B],^[a] [tcm_3B]^[b] and [tcb_4B]^[c] as [EMIm]⁺ (1-ethyl-3-methylimidazolium) salt.

	3	7	[dca_2B] ^[d]	[tcm_3B] ^[d]	[tcb_4B] ^[d]
$^{11}\text{B}\{^1\text{H}\}$	–	$-9.9^{\text{[e]}}$	$-11.8^{\text{[f]}}$	$-10.1^{\text{[f]}}$	$-8.5^{\text{[f]}}$
Raman	2164,	2268	2365	2297, ^[g]	2323
ν_{CN}	2172 ^[g]			2353	
$d(\text{C}-\text{N})^{\text{[h]}}$	1.151(2)	1.136(8)	1.135(6)	1.138(3)	1.136(2)

[a] $[(\text{NC})\text{B}(\text{C}_6\text{F}_5)_3]^-$. [b] $[\text{C}[\text{CN}\cdot\text{B}(\text{C}_6\text{F}_5)_3]_3]^-$. [c] $[\text{B}(\text{CN}\cdot\text{B}(\text{C}_6\text{F}_5)_3)_4]^-$. [d] From Reference.^[34] [e] In CD_2Cl_2 . [f] In CDCl_3 . [g] Most intense. [h] Average.

8 undergoes reaction with acetonitrile which can be observed nicely with $^{11}\text{B}\{^1\text{H}\}$ NMR. At room temperature a broad and low-field shifted resonance at -11.3 and a sharper signal at -22 ppm ($\Delta\nu_{1/2} = 100$ Hz) are observed. When the temperature is increased, the first resonance can be recognized as a superposition of two distinct signals at -11.3 and -12.2 ppm (see ESI Figure S39). Cleavage of the N–B donor–acceptor bonds of **8**

results in formation of the borane- $[\text{D}_3]$ acetonitrile adduct $\text{CD}_3\text{CN}-\text{B}(\text{C}_6\text{F}_5)_3$, which can be assigned to the most low-field shifted resonance at -11.3 ppm (cf. -10.3 ppm in benzene).^[30] The signals at -12.2 and -22 ppm can be assigned to $[(\text{C}_6\text{F}_5)_3\text{B}(\mu\text{-CN})\cdot\text{B}(\text{C}_6\text{F}_5)_3]^-$, which is in good accordance with values known from the literature.^[32,33] This means that at least one CN ligand is abstracted from the $[\text{Si}(\text{CN})_6]$ scaffold, which could lead to the formation of $[\text{Si}(\text{CN})_5]^-$ and lower substituted silicon species. However, no new signals for any of these species could be observed by means of $^{13}\text{C}\{^1\text{H}\}$ and $^{29}\text{Si}\{\text{IG}\}$ NMR and no product material could be isolated from the reaction mixture so far.

N–B-bond cleavage was also noticed when the sample was analyzed by (ESI-TOF)-MS due to the reaction with the column eluent methanol. As a result, new ions were detected with $m/z = 529$ and 543 for $[\text{B}(\text{C}_6\text{F}_5)_3\text{OH}]^-$ and $[\text{B}(\text{C}_6\text{F}_5)_3(\text{OMe})]^-$, respectively. The Raman spectrum of **8** shows a single sharp resonance at 2268 cm^{-1} for the ν_{CN} vibration. The signal is shifted to higher wavenumbers with respect to **3** at 2172 cm^{-1} (strongest), indicating a strengthening of the CN triple bond. The band is located in the similar region as for the cyanidoborates mentioned above (Table 2). However, no band could be detected by means of IR analysis for ν_{CN} stretching vibrations.

Structure Elucidation

The colorless, block-shaped crystals of solvent-free $\text{K}_2[\text{Si}(\text{CN})_6]$ crystallizes isotypically to known $\text{Li}_2[\text{Si}(\text{CN})_6]\cdot 2\text{H}_2\text{O}$ ^[28] in the trigonal space group $P\bar{3}m1$ with one formula unit per cell, shown in Figure 1. The octahedral $[\text{Si}(\text{CN})_6]^{2-}$ ion coordinates to twelve different K^+ ions (each N atom to two K^+ ions), while the slightly distorted octahedrally surrounded K^+ ion is linked to N atoms of cyanide ligands of six different adjacent $[\text{Si}(\text{CN})_6]^{2-}$ ions (Figure 1, top). Main motifs in the crystal structure are planar four-membered K_2N_2 assemblies, twelve-membered $\text{K}_2\text{Si}_2(\text{CN})_4$ entities in chair conformation, connecting two different $[\text{Si}(\text{CN})_6]^{2-}$ ions, and bent eight-membered $\text{K}_2\text{NSi}(\text{CN})_2$ units, building a 3D network (Figure 1, bottom). The Si–C bonds are in the expected range [$d(\text{Si}-\text{C}) = 1.9506(8)$ Å, cf. $\Sigma r_{\text{cov.}}(\text{Si}-\text{C}) = 1.91$ Å],^[35] while the $\text{K}\cdots\text{N}$ contacts with $2.836(1)$ Å are slightly elongated compared to the sum of the covalent radii [cf. $\Sigma r_{\text{cov.}}(\text{K}-\text{N}) = 2.67$ Å]^[35] and shortened compared to the $\text{K}\cdots\text{N}$ distance in KCN with 3.00 Å.^[36]

All imidazolium hexacyanidosilicates crystallize as block-shaped and colorless crystals. Only weak anion \cdots cation contacts, built by C–H \cdots N hydrogen bonds, were found in all structures according to single-crystal X-ray analysis [heavy atom distances, shortest given $d(\text{C}_{\text{cation}}\cdots\text{N}_{\text{anion}})$ [Å]: **6** $3.151(4) \approx$ **4** $3.161(3) \approx$ **3** $3.173(2) <$ **5** $3.199(3) <$ **1** $3.291(2) <$ **2** $3.331(2)$ Å]. No cation \cdots cation contacts were found in the imidazolium salts **1**, **2** and **6**, therefore no coordination polymer in the crystal was recognized. Interestingly, only in the structures of compound **3** and **4**, π - π -stacking of the substituted phenyl rings of the imidazolium cations in adjacent planes can be observed. In **3** a parallel-displaced and in **4** a sandwich conformation is found with centroid-to-centroid distances of $4.2929(5)$ Å and $3.7882(4)$ Å, respectively. These interactions lead to a wave-

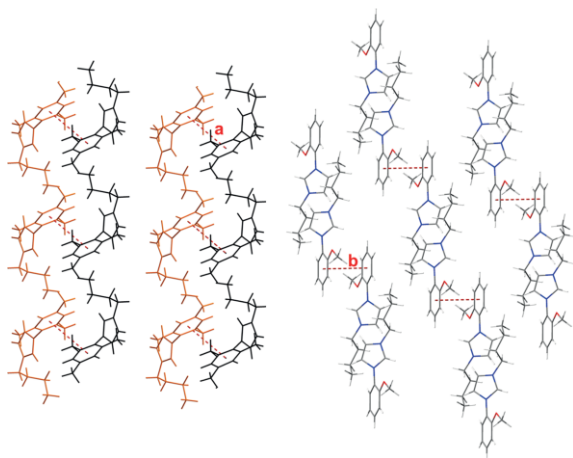


Figure 2. Wires-and-sticks representations of a section of the crystal structures of **3** (left) and **4** (right). The $[\text{Si}(\text{CN})_6]^{2-}$ ions are omitted for reasons of clarity. View along the a -axis (both). Selected centroid-to-centroid distances [Å]: **a** = 4.2929(5), **b** = 3.7882(4).

shaped pattern in **3** or to a step-shaped arrangement in **4** of the cations in the crystal structure (Figure 2).

In the 2,4-difluoro-substituted compound **5**, a layered motif (**ABAB**) is formed in the crystal structure, stabilized by C–H...F hydrogen bonds which are formed between adjacent imidazolium cations (Figure 3). The *para*-F atoms are exclusively connected to a imidazolium ring in the same layer [**e**: $d(p\text{-F}-\text{C}) = 3.106(3)$ Å], while the *ortho*-F atoms are linked to a butyl chain [**c**: $d(o\text{-F}-\text{C}) = 3.329(3)$ Å] of an adjacent imidazolium cation in the same layer and also to the C–H-acidic position of a cation in a second one [**d**: $d(o\text{-F}-\text{C}) = 3.251(2)$ Å].

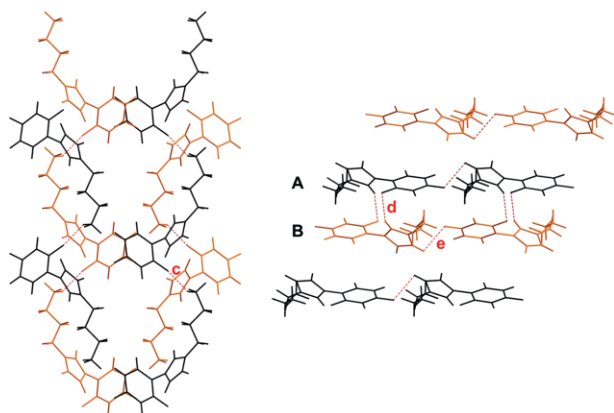


Figure 3. Wires-and-sticks representations of a section of the crystal structures of **5**. View along a -axis (left) and b -axis (right). The $[\text{Si}(\text{CN})_6]^{2-}$ ions are omitted for clarity. Selected distances in Å, heavy-atom distance in the H-bridges: **c** F1–C16 3.329(3), **d** F1–C4 3.251(2), **e** F2–C6 3.106(3).

$[\text{Mes}(n\text{Bu})\text{Im}]_2[\text{Si}[(\text{CN})\text{B}(\text{C}_6\text{F}_5)_3]_6] \cdot 6\text{CH}_2\text{Cl}_2$ (**7**) crystallizes in the triclinic space group $P\bar{1}$ with one formula unit per cell. The octahedral $[\text{Si}(\text{CN})_6]$ core links via the N atoms to six $\text{B}(\text{C}_6\text{F}_5)_3$ molecules, forming a bulky, spherical anion (Figure 4). Due to the poor quality of the data ($wR_2 = 33\%$), we would like to point out that a discussion regarding to structural parameter such as bond length and angles should be handled with care. However, the N–B donor-acceptor bonds are in the range of a covalent

single bond [$d(\text{N}-\text{B}) = 1.598(1)$ Å (average), cf. $\Sigma r_{\text{cov.}}(\text{N}-\text{B}) = 1.56$ Å]^[35] and of similar strength compared to the N–B bond(s) in $\text{CH}_3\text{CN}-\text{B}(\text{C}_6\text{F}_5)_3$ with 1.616(3) Å,^[30] $\text{HCN}-\text{B}(\text{C}_6\text{F}_5)_3$ with 1.606(3) Å^[37] or in $[\text{B}[(\text{CN})\cdot\text{B}(\text{C}_6\text{F}_5)_3]_4]^-$ with 1.606(2) Å (average),^[34] as the structural data clearly demonstrate. The C–N triple bond with 1.136(8) Å (average) is shortened compared to the C–N distance in **3** that nicely correlates to observations of Raman analyses (Table 2). The cyanide ligands are slightly bent away from the Si center with $(\text{Si}-\text{C}-\text{N}) = 173.3(6)^\circ$, $172.3(6)^\circ$, $175.2(5)^\circ$ [cf. $178.1(1)^\circ$ (average) in **3**], probably due to the steric stress and the electrostatic repulsion of the F atoms between the bulky $\text{B}(\text{C}_6\text{F}_5)_3$ molecules [$d(\text{F}\cdots\text{F}) = 2.78(1)$ Å (shortest)]. Weak anion...cation interactions can be considered, formed by C–H...F hydrogen bonds between the anion and different H atoms ("at-oms" ist merkwürdig getrennt im gedruckten Text) of the $[\text{Mes}(n\text{Bu})\text{Im}]^+$ ion [non-hydrogen atom distances and only A-layer of the disorder is discussed: $(\text{F}\cdots\text{C}_{\text{alkyl}})$: 3.24(2), 3.27(3), 3.39(2); $(\text{F}\cdots\text{C}_{\text{Mes}})$: 3.09(2), 3.28(3); $(\text{F}\cdots\text{C}_{\text{Im}})$: 3.00(2) Å].

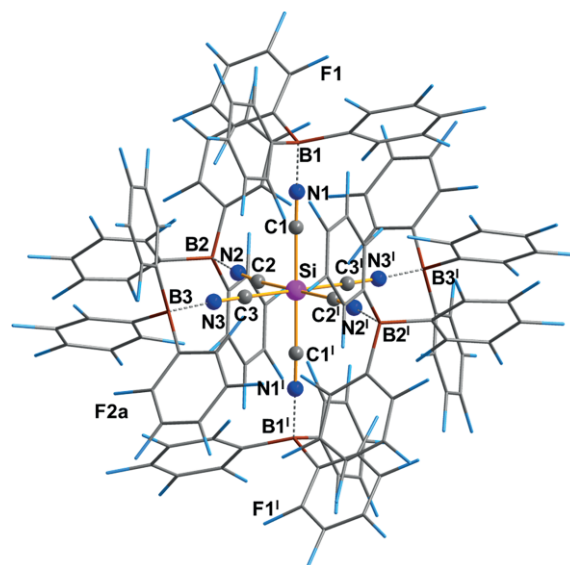


Figure 4. Molecular structure of the $[\text{Si}[(\text{CN})\text{B}(\text{C}_6\text{F}_5)_3]_6]^{2-}$ anion in the crystal structure of **7**. The $[\text{Si}(\text{CN})_6]$ -core is represented as ball-and-stick model, while the $\text{B}(\text{C}_6\text{F}_5)_3$ molecules are shown as wires-and-sticks model. The $[\text{Mes}(n\text{Bu})\text{Im}]^+$ cations, as well as disorders, are omitted for reasons of clarity. Selected bond lengths [Å] and angles $^\circ$: Si–C1 1.958(6), Si–C2 1.945(6), Si–C1 1.957(7), C1–N1 1.138(7), C2–N2 1.137(8), C3–N3 1.131(9), N1–B1 1.608(8), N2–B2 1.589(9), N3–B3 1.597(9); Si–C1–N1 172.3(6), Si–C2–N2 173.3(6), Si–C3–N3 175.2(5), C1–Si–C1' 180.0, C1–Si–C2' 90.1(3). Symmetry code: (I) 1 – x , 1 – y , 1 – z .

Conclusion

In conclusion, we present facile salt metathesis reactions of $\text{K}_2[\text{Si}(\text{CN})_6]$ with different substituted imidazolium bromides of the type $[\text{R}-\text{Ph}(n\text{Bu})\text{Im}]\text{Br}$, leading to imidazolium hexacyanidosilicate salts in moderate yields (43–69%), which decompose at elevated temperatures and thus cannot be regarded as ILs. X-ray structure elucidation of the solvent-free $\text{K}_2[\text{Si}(\text{CN})_6]$ revealed the formation of a 3D network. The crystal structures of the imidazolium hexacyanidosilicates show depending on the substituents either well-separated molecular ions (**1**, **2** and **6**) or

have structural motifs like a wave-shaped (**3**) or stepped (**4**) arrangement due to π - π interactions of the phenyl system. In case of **5** the cations are arranged in ABAB layers, stabilized by intermolecular F...H hydrogen bridges. The reaction of the Lewis acidic borane $B(C_6F_5)_3$ with the $[Si(CN)_6]^{2-}$ dianion led to complete functionalization of the cyanide ligands and the voluminous $\{Si[(CN)B(C_6F_5)_3]_6\}^{2-}$ anion in form of its $[Mes(nBu)Im]^+$ salt was obtained. The compound is only sparingly soluble in CH_2Cl_2 and readily decomposes under N-B bond cleavage when polar solvents such as CH_3CN or MeOH are used. This new anion could possibly be used as a very bulky, weakly coordinating anion when it is combined with transition metals and could increase its catalytic activity due to reduced ion pairing.

Experimental Section

Caution! TMS-CN is highly toxic! Appropriate safety precautions (HCN detector, gas mask, low temperature) should be taken. Experimental spectra and additional crystal structure representations can be found in the Supporting Information.

General Information: All manipulations were carried out in oxygen- and moisture-free conditions in an argon atmosphere using standard Schlenk or dry-box techniques if not mentioned otherwise.

NMR spectra were recorded on Bruker spectrometers (AVANCE 250, AVANCE 300 or AVANCE 500) and were referenced internally to the deuterated solvent (^{13}C : CD_2Cl_2 $\delta_{ref} = 54.0$ ppm, CD_3CN $\delta_{ref,1} = 1.3$ ppm, $\delta_{ref,2} = 118.3$ ppm), to protic impurities in the deuterated solvent (1H : $CHDCl_2$ $\delta_{ref} = 5.32$ ppm, CHD_2CN $\delta_{ref} = 1.94$ ppm)^[38] or externally (^{19}F : $CFCl_3$ $\delta_{ref} = 0$ ppm, ^{29}Si : $SiMe_4$ $\delta_{ref} = 0$ ppm). All measurements were carried out at ambient temperature unless denoted otherwise. IR spectra were recorded with a Bruker Alpha II FT-IR spectrometer with ATR device. For Raman spectroscopy a LabRAM HR 800 Horiba Jobin YVON equipped with an Olympus BX41 microscope with variable lenses were used. The samples were excited by a red laser (633 nm, 17 mW, air-cooled HeNe laser), a green laser (532 nm, 50 mW, air-cooled, frequency-doubled Nd:YAG solid-state laser) or a blue laser (473 nm, 20 mW, air-cooled solid-state laser). All measurements were carried out at ambient temperature unless stated otherwise. CHN analyses were recorded using an Elementar vario Micro cube CHNS analyser. For TGA, samples were analyzed using a Setaram Instrumentation Labsys analyzer. Melting points (uncorrected) were measured with a Stanford Research Systems [heating rate 5 K min^{-1} (clearing-points are reported)]. Mass spectra were recorded with a Xevo G2-XS TOF system coupled with a LC from Waters or with an Agilent Technologies 6130 Quadrupole system coupled with a LC from Agilent Technologies 1260 Infinity system.

X-ray Structure Determination: X-ray quality crystals of all compounds were selected in Kel-F-oil (Riedel de Haen) at ambient temperatures. Single crystals were measured on a Bruker D8 Quest or a Bruker Apex Kappa II CCD diffractometer using graphite-monochromated $Mo-K_{\alpha}$ radiation ($\lambda = 0.71073$). The structures were solved by iterative methods (SHELXT)^[39] and refined by full-matrix least-squares procedures (SHELXL).^[40] Semi-empirical absorption corrections were applied (SADABS).^[41] All non-hydrogen atoms were refined anisotropically and hydrogen atoms were included in the refinement at calculated positions using a riding model.

Deposition Numbers 1984754 – 1984761 contain the supplementary crystallographic data for this paper. These data are provided

free of charge by the joint Cambridge Crystallographic Data Centre and Fachinformationszentrum Karlsruhe Access Structures service www.ccdc.cam.ac.uk/structures.

Compound Syntheses: Bromide salts $[R-Ph(nBu)Im]Br$ with $R = 2-Me, 4-Me, 2,4,6-Me$ and $2-MeO$ were prepared according to the literature.^[25–27,42] The synthesis of the starting compounds $K_2[Si(CN)_6]$, $[2,4-FPh(nBu)Im]Br$ and $[4-BrPh(nBu)Im]Br$ can be found in the supporting information.

General Synthesis of Imidazolium Hexacyanidosilicates (1–6): $K_2[Si(CN)_6]$ (1 equiv.) and $[R-Ph(nBu)Im]Br$ (2 equiv.) were placed in a Schlenk-flask. The solids were suspended in 50 mL of acetonitrile and stirred for 16 hours at room temperature. The suspension was filtered with a glass frit and acetonitrile was removed in vacuo.

[2-MePh(nBu)Im] $_2$ [Si(CN) $_6$] (1): 0.9 g (3.4 mmol) of potassium hexacyanidosilicate and 1.9 g (6.8 mmol, 2 equiv.) of $[2-MePh(nBu)Im]Br$ was used. The product was crystallized from a mixture of acetonitrile and CH_2Cl_2 at -30 °C leading to formation of colorless crystals in yields of 67 % (1.4 g, 2.2 mmol). $T_{dec.} = 164$ °C. EA % calcd. (found) %: C 66.42 (65.51); H 6.23 (5.81); N 22.78 (22.24). (ESI)-MS (m/z) pos.: 215 ($[2-MePh(nBu)Im]^+$); neg.: 106 ($[Si(CN)_3]^-$); 158 ($[Si(CN)_5]^-$). 1H NMR (300 K, CD_3CN , 250.13 MHz): $\delta = 0.99$ (t, 6H, CH_2CH_3 , $^3J(^1H-^1H) = 7.3$ Hz), 1.33–1.51 (m, 4H, CH_2CH_3), 1.92–2.01 (m, 4H, CH_2CH_2), 2.23 (s, 6H, Ph- CH_3), 4.28 (t, 4H, NCH_2 , $^3J(^1H-^1H) = 7.3$ Hz), 7.38–7.55 (m, 8H, C_{Aryl}), 7.55–7.60 (m, 2H, $NCHCHN-nBu$), 7.62–7.67 (m, 2H, $NCHCHN-nBu$), 8.67–8.71 (m, 2H, $NCHN$). $^{13}C\{^1H\}$ NMR (300 K, CD_3CN , 62.9 MHz): $\delta = 13.7$ (s, CH_2CH_3), 17.5 (s, $o-CH_3$), 20.1 (s, CH_2CH_3), 32.4 (s, CH_2CH_2), 50.8 (s, NCH_2), 123.7 (s, $NCHCHN-nBu$), 125.0 (s, $NCHCHN-nBu$), 127.5 (s, C_{Aryl}), 128.4 (s, C_{Aryl}), 132.0 (s, C_{Aryl}), 132.7 (s, C_{Aryl}), 134.9 (s, *ipso*-CN), 135.2 (s, C_{Aryl}), 137.0 (s, $NCHN$), 140.0 (s, $Si(CN)_6$). ^{29}Si (IG) NMR (300 K, CD_3CN , 99.3 MHz) not observed ($Si(CN)_6$). IR (ATR, 298 K, 32 scans, cm^{-1}): $\tilde{\nu} = 420$ (w), 441 (w), 451 (w), 464 (w), 569 (vs), 624 (vw), 637 (vw), 655 (w), 678 (vw), 717 (w), 750 (w), 762 (m), 775 (w), 800 (vw), 824 (vw), 859 (w), 884 (vw), 958 (vw), 1026 (vw), 1047 (vw), 1076 (w), 1121 (w), 1191 (m), 1212 (w), 1249 (vw), 1271 (vw), 1300 (vw), 1337 (vw), 1368 (vw), 1381 (vw), 1391 (vw), 1416 (vw), 1449 (w), 1461 (w), 1494 (w), 1554 (w), 1568 (w), 1636 (vw), 1655 (vw), 1714 (vw), 2166 (vw), 2875 (vw), 2932 (vw), 2961 (w), 3093 (w), 3118 (vw), 3126 (vw), 3140 (w). Raman (laser: 633 nm, accumulation time: 4 s, 16 scans, 298 K, cm^{-1}): $\tilde{\nu} = 71$ (4), 80 (6), 105 (6), 145 (6), 194 (1), 277 (1), 306 (1), 322 (1), 369 (0), 406 (1), 453 (1), 468 (2), 549 (2), 554 (2), 627 (1), 656 (1), 659 (1), 682 (1), 718 (1), 752 (1), 801 (2), 825 (1), 885 (1), 962 (3), 999 (1), 1028 (1), 1046 (2), 1078 (1), 1120 (1), 1161 (1), 1212 (1), 1250 (1), 1274 (1), 1307 (1), 1338 (1), 1359 (1), 1372 (2), 1391 (1), 1419 (2), 1436 (1), 1448 (1), 1464 (1), 1497 (1), 1556 (1), 1585 (1), 1610 (1), 2118 (1), 2164 (3), 2171 (10), 2735 (1), 2875 (2), 2915 (2), 2933 (3), 2966 (3), 2989 (1), 3009 (1), 3068 (2), 3081 (2), 3130 (2), 3158 (1).

[4-MePh(nBu)Im] $_2$ [Si(CN) $_6$] (2): 0.5 g (1.9 mmol) of the potassium hexacyanidosilicate and 1.8 g (3.8 mmol, 2 equiv.) of $[4-MePh(nBu)Im]Br$ was used. The product was crystallized from CH_2Cl_2 leading to formation of colorless crystals in yields of 55 % (0.7 g, 1.1 mmol). $T_{dec.} = 119$ °C. EA % calcd. (found) %: C 66.42 (66.19); H 6.23 (6.23); N 22.78 (22.65). (ESI)-MS (m/z) pos.: 215 ($[4-MePh(nBu)Im]^+$); neg.: 106 ($[Si(CN)_3]^-$); 158 ($[Si(CN)_5]^-$). 1H NMR (300 K, CD_3CN , 300.13 MHz): $\delta = 0.98$ (t, 6H, CH_2CH_3 , $^3J(^1H-^1H) = 7.4$ Hz), 1.35–1.48 (m, 4H, CH_2CH_3), 1.87–2.00 (m, 4H, CH_2CH_2), 2.43 (s, 6H, *ph-CH*), 4.26 (t, 4H, NCH_2 , $^3J(^1H-^1H) = 7.4$ Hz), 7.40–7.47 (m, 4H, *m-CH*), 7.41–7.55 (m, 4H, *o-CH*), 7.59–7.60 (m, 2H, $NCHCHN-nBu$), 7.74–7.75 (m, 2H, $NCHCHN-nBu$), 8.98–9.03 (m, 2H, $NCHN$). $^{13}C\{^1H\}$ NMR (300 K, CD_3CN , 75.5 MHz): $\delta = 13.7$ (s, CH_2CH_3), 20.0 (s, CH_2CH_3), 21.1 (s, $Ph-CH_3$), 32.4 (s, CH_2CH_2), 50.8 (s, NCH_2), 122.7

(s, NCHCHN-*n*Bu), 123.2 (s, *m*-CH) 124.1 (s, NCHCHN-*n*Bu), 131.7 (s, *o*-CH), 133.5 (s, *ipso*-CN), 135.4 (s, NCHN), 140.0 (s, Si(CN)₆) 141.7 (w, *ipso*-C_{para}). ²⁹Si(IG) NMR(300 K, CD₃CN, 99.3 MHz) not observed (Si(CN)₆). IR (ATR, 298 K, 32 scans, cm⁻¹): $\tilde{\nu}$ = 422 (w), 437 (w), 464 (w), 530 (s), 569 (vs), 639 (w), 657 (w), 705 (vw), 721 (vw), 742 (w), 773 (m), 800 (vw), 816 (m), 830 (w), 857 (w), 884 (vw), 907 (vw), 958 (vw), 1020 (vw), 1047 (vw), 1078 (w), 1117 (w), 1125 (vw), 1205 (m), 1236 (vw), 1271 (vw), 1300 (vw), 1333 (vw), 1381 (w), 1414 (vw), 1459 (w), 1471 (w), 1510 (w), 1556 (w), 1568 (w), 1638 (vw), 1651 (vw), 1710 (vw), 1904 (vw), 2164 (vw), 2875 (w), 2932 (w), 2955 (w), 2965 (vw), 3097 (w), 3118 (vw), 3142 (w). Raman (laser: 633 nm, accumulation time: 4 s, 20 scans, 298 K, cm⁻¹): $\tilde{\nu}$ = 80 (5), 89 (5), 143 (4), 237 (1), 270 (1), 292 (1), 302 (1), 326 (1), 341 (1), 361 (1), 385 (1), 406 (1), 467 (2), 531 (1), 607 (1), 629 (1), 640(1), 658 (1), 706 (1), 722 (1), 775 (1), 800 (3), 818 (1), 831 (1), 859 (1), 908 (1), 959 (5), 1009 (1), 1021 (1), 1033 (1), 1079 (1), 1117 (1), 1183 (2), 1206 (1), 1218 (1), 1265 (1), 1272 (1), 1302 (1), 1309 (1), 1334 (1), 1370 (1), 1380 (1), 1414 (2), 1446 (1), 1463 (1), 1473 (1), 1513 (1), 1558 (1), 1571 (1), 1612 (1), 2117 (1), 2123 (1), 2164 (2), 2171 (10), 2742 (1), 2873 (1), 2929 (1), 2949 (1), 2964 (1), 2990 (1), 3017 (1), 3046 (1), 3075 (2), 3130 (1), 3155 (1).

[Mes(*n*Bu)Im]₂[Si(CN)₆] (3): 0.8 g (3.0 mmol) of the potassium hexacyanidosilicate and 1.9 g (6.1 mmol, 2 equiv.) of [Mes(*n*Bu)Im]Br was used. The product was crystallized from a mixture of diethyl ether and CH₂Cl₂ at -30 °C leading to formation of colorless crystals in yields of 54 % (1.1 g, 1.6 mmol). *T*_{dec.} = 146 °C. EA % calcd. (found) %: C 68.03 (68.37); H 6.91 (7.54); N 20.88 (20.75). (ESI)-MS (*m/z*) pos.: 243 ([Mes(*n*Bu)Im]⁺); neg.: 106 ([Si(CN)₃]⁻); 158 ([Si(CN)₅]⁻). ¹H NMR (298.5 K, CD₃CN, 300.13 MHz): δ = 0.98 (t, 6H, CH₂CH₃, ³J(¹H-¹H) = 7.2 Hz), 1.32–1.44 (m, 4H, CH₂CH₃), 1.94–1.98 (m, 4H, CH₂CH₂), 2.04 (s, 12H, *o*-CH₃), 2.36 (s, 6H, *p*-CH₃), 4.27–4.32 (m, 4H, NCH₂), 7.12 (s, 4H, *m*-CH), 7.44–7.47 (m, 2H, NCHCHN-*n*Bu), 7.66–7.69 (m, 2H, NCHCHN-*n*Bu), 8.60–8.66 (m, 2H, NCHN). ¹³C{¹H} NMR (298.5 K, CD₃CN, 75.5 MHz): δ = 13.7 (s, CH₂CH₃), 17.4 (s, *o*-CH₃), 20.0 (s, CH₂CH₃), 21.1 (s, *p*-CH₃), 32.2 (s, CH₂CH₂), 50.9 (s, NCH₂), 124.2 (s, NCHCHN-*n*Bu), 125.1 (s, NCHCHN-*n*Bu) 130.4 (s, *ipso*-C_{ortho}), 132.0 (s, *ipso*-C_{para}), 135.7 (s, *m*-CH), 137.2 (s, NCHN), 140.0 (s, Si(CN)₆) 142.2 (s, *ipso*-CN). ²⁹Si(IG) NMR (300 K, CD₃CN, 99.3 MHz) not observed (Si(CN)₆). IR (ATR, 298 K, 32 scans, cm⁻¹): $\tilde{\nu}$ = 431 (m), 569 (vs), 641 (w), 672 (m), 732 (w), 754 (m), 818 (vw), 849 (w), 861 (w), 894 (vw), 936 (vw), 968 (vw), 1018 (vw), 1039 (w), 1067 (w), 1088 (w), 1119 (vw), 1158 (w), 1203 (w), 1292 (vw), 1329 (vw), 1381 (w), 1442 (w), 1461 (w), 1484 (w), 1548 (w), 1566 (w), 1609 (w), 2168 (vw), 2862 (w), 2875 (vw), 2934 (w), 2959 (w), 3093 (vw), 3142 (w), 3165 (vw). Raman (laser: 633 nm, accumulation time: 12 s, 25 scans, 298 K, cm⁻¹): $\tilde{\nu}$ = 96 (10), 148 (4), 235 (2), 320 (2), 335 (2), 352 (1), 408 (2), 445 (1), 467 (2), 501 (1), 512 (1), 556 (1), 577 (4), 821 (1), 893 (1), 946 (1), 970 (3), 1020 (1), 1059 (1), 1070 (1), 1090 (2), 1263 (1), 1297 (1), 1331 (2), 1364 (2), 1374 (2), 1380 (2), 1415 (3), 1442 (2), 1551 (2), 1568 (1), 1611 (2), 2120 (2), 2164 (5), 2172 (10), 2736 (2), 2865 (3), 2878 (3), 2924 (5), 2941 (4), 2957 (3), 2968 (3), 2971 (3), 2976 (3), 2999 (3), 3007 (3), 3010 (3), 3014 (3), 3022 (3), 3026 (3), 3033 (3), 3077 (2), 3080 (2), 3083 (2), 3113 (2), 3117 (2), 3146 (3), 3149 (3), 3168 (3).

[2-MeOPh(*n*Bu)Im]₂[Si(CN)₆] (4): 0.5 g (1.9 mmol) of potassium hexacyanidosilicate and 1.2 g (3.9 mmol, 2 equiv.) of [2-MeOPh(*n*Bu)Im]Br was used. The product was crystallized from CH₂Cl₂ at room temperature leading to formation of colorless crystals in yields of 55 % (0.7 g, 1.1 mmol). *T*_{dec.} = 125 °C. EA % calcd. (found) %: C 63.13 (62.75); H 5.92 (6.37); N 21.65 (21.39). (ESI)-MS(*m/z*) pos.: 231 ([2MeOPh(*n*Bu)Im]⁺); neg.: 106 ([Si(CN)₃]⁻); 158 ([Si(CN)₅]⁻). ¹H NMR (300 K, CD₃CN, 250.13 MHz): δ = 1.00 (t, 6H, CH₂CH₃, ³J(¹H-¹H) = 7.4 Hz), 1.34–1.52 (m, 4H, CH₂CH₃), 1.95–2.00

(m, 4H, CH₂CH₂), 3.94 (s, 6H, OCH₃), 4.30 (t, 4H, NCH₂, ³J(¹H-¹H) = 7.3 Hz), 7.14–7.36 (m, 4H, CH_{Ar}), 7.48–7.65 (m, 4H, CH_{Ar}), 7.59–7.62 (m, 2H, NCHCHN-*n*Bu), 7.66–7.71 (m, 2H, NCHCHN-*n*Bu), 8.84–8.91 (m, 2H, NCHN). ¹³C{¹H} NMR (300 K, CD₃CN, 75.5 MHz): δ = 13.7 (s, CH₂CH₃), 20.0 (s, CH₂CH₃), 32.4 (s, CH₂CH₂), 50.8 (s, NCH₂), 57.1 (s, OCH₃), 114.1 (s, C_{Ar}), 122.2 (s, C_{Ar}), 123.1 (s, C_{Ar}), 124.5 (s, *ipso*-CN), 124.6 (s, NCHCHN-*n*Bu), 126.7 (s, C_{Ar}), 132.8 (s, NCHCHN-*n*Bu), 137.3 (s, NCHN), 140.0 (s, Si(CN)₆), 153.4 (s, COCH₃). ²⁹Si(IG) NMR (300 K, CD₃CN, 99.3 MHz) not observed (Si(CN)₆). IR (ATR, 198 K, 32 scans, cm⁻¹): $\tilde{\nu}$ = 424 (m), 476 (w), 530 (m), 567 (vs), 628 (w), 651 (w), 668 (w), 723 (w), 754 (m), 769 (m), 791 (w), 861 (w), 958 (w), 979 (vw), 1020 (m), 1047 (vw), 1065 (w), 1107 (w), 1125 (w), 1162 (w), 1185 (m), 1197 (w), 1257 (m), 1286 (w), 1302 (w), 1335 (w), 1379 (w), 1422 (vw), 1440 (w), 1461 (w), 1471 (w), 1502 (m), 1554 (w), 1566 (w), 1605 (w), 1933 (vw), 2166 (vw), 2359 (vw), 2846 (vw), 2862 (vw), 2879 (vw), 2941 (w), 2963 (w), 3107 (w), 3140 (w), 3151 (w). Raman (laser: 532 nm, accumulation time: 3 s, 13 scans, 298 K, cm⁻¹): $\tilde{\nu}$ = 129 (4), 346 (1), 411 (1), 465 (2), 794 (4), 885 (4), 959 (4), 985 (4), 1024 (5), 1047 (5), 1163 (5), 1261 (6), 1336 (6), 1361 (6), 1383 (6), 1423 (7), 1461 (7), 1500 (6), 1553 (7), 1595 (8), 2055 (7), 2163 (8), 2167 (8), 2176 (10), 2511 (7), 2851 (6), 2939 (6), 2961 (6), 3087 (6), 3163 (6).

[2,4-FPh(*n*Bu)Im]₂[Si(CN)₆] (5): 0.8 g (2.9 mmol) of potassium hexacyanidosilicate and 1.9 g (5.9 mmol, 2 equiv.) of [2,4-FPh(*n*Bu)Im]Br was used. The product was crystallized from acetonitrile at room temperature leading to formation of colorless crystals in yields of 43 % (0.8 g, 1.3 mmol). *T*_{dec.} = 96 °C. EA % calcd. (found) %: C 58.35 (57.46); H 4.59 (4.73); N 21.26 (20.77). (ESI)-MS (*m/z*) pos.: 237 ([2,4Ph(*n*Bu)Im]⁺); neg.: 106 ([Si(CN)₃]⁻); 158 ([Si(CN)₅]⁻). ¹H NMR (298.1 K, CD₃CN, 300.13 MHz): δ = 1.00 (t, 6H, CH₂CH₃, ³J(¹H-¹H) = 7.5 Hz), 1.39–1.47 (m, 4H, CH₂CH₃), 1.95–2.00 (m, 4H, CH₂CH₂), 4.31 (t, 4H, NCH₂, ³J(¹H-¹H) = 7.3 Hz), 7.24–7.30 (m, 2H, *m*-CH), 7.31–7.37 (m, 2H, CFCHCF), 7.65–7.68 (m, 2H, NCHCHN-*n*Bu), 7.70–7.72 (m, 2H, NCHCHN-*n*Bu), 7.72–7.78 (m, 2H, *o*-CH), 8.88–8.97 (m, 2H, NCHN). ¹³C{¹H} NMR (298.1 K, CD₃CN, 75.5 MHz): δ = 13.7 (s, CH₂CH₃), 20.0 (s, CH₂CH₃), 32.3 (s, CH₂CH₂), 51.0 (s, NCH₂), 106.7 (dd, FCCHCF, ²J(¹³C-¹⁹F) = 24 Hz, ²J(¹³C-¹⁹F) = 28 Hz), 113.9 (dd, *m*-CH, ²J(¹³C-¹⁹F) = 4 Hz, ⁴J(¹³C-¹⁹F) = 23 Hz), 120.6 (dd, *ipso*-CN, ²J(¹³C-¹⁹F) = 4 Hz, ²J(¹³C-¹⁹F) = 11 Hz), 124.0 (s, NCHCHN-*n*Bu), 124.6 (s, NCHCHN-*n*Bu), 129.2 (d, *o*-CH, ³J(¹³C-¹⁹F) = 11 Hz), 137.4 (br, NCHN), 140.1 (s, Si(CN)₆), 156.8 (dd, *o*-CF, ³J(¹³C-¹⁹F) = 13 Hz, ¹J(¹³C-¹⁹F) = 254 Hz), 164.5 (dd, *p*-CF, ³J(¹³C-¹⁹F) = 12 Hz, ¹J(¹³C-¹⁹F) = 252 Hz). ¹⁹F{¹H} NMR (298.1 K, CD₃CN, 282.37 MHz) δ = -120.5 (d, 1F, CF, ⁴J(¹⁹F-¹⁹F) = 9 Hz), -106.8 (d, 1F, CF, ⁴J(¹⁹F-¹⁹F) = 9 Hz). ²⁹Si(IG) NMR (300 K, CD₃CN, 99.3 MHz) not observed (Si(CN)₆). IR (ATR, 298 K, 32 scans, cm⁻¹): $\tilde{\nu}$ = 429 (m), 482 (m), 509 (m), 571 (vs), 604 (w), 616 (w), 628 (w), 653 (w), 707 (vw), 721 (vw), 738 (w), 777 (m), 802 (vw), 822 (m), 843 (m), 851 (m), 907 (vw), 944 (w), 975 (m), 1014 (vw), 1032 (vw), 1074 (m), 1105 (m), 1121 (w), 1142 (m), 1185 (m), 1195 (m), 1218 (w), 1236 (w), 1271 (m), 1298 (vw), 1348 (w), 1366 (vw), 1383 (w), 1445 (w), 1461 (w), 1506 (m), 1558 (m), 1572 (w), 1611 (w), 1618 (w), 2172 (vw), 2866 (vw), 2879 (vw), 2938 (w), 2965 (w), 3079 (vw), 3112 (w), 3136 (w), 3149 (w). Raman (laser: 473 nm, accumulation time: 4 s, 13 scans, 298 K, cm⁻¹): $\tilde{\nu}$ = 162 (2), 247 (3), 270 (2), 319 (2), 355 (3), 414 (3), 431 (3), 467 (3), 569 (3), 742 (5), 947 (4), 977 (5), 1032 (4), 1074 (4), 1119 (4), 1274 (4), 1348 (5), 1367 (6), 1415 (6), 1511 (5), 1561 (5), 1619 (6), 2173 (9), 2179 (10), 2880 (8), 2904 (8), 2925 (8), 2942 (8), 2967 (8), 2973 (8), 2986 (8), 3092 (9), 3111 (8), 3132 (7), 3138 (7), 3149 (7), 3160 (8).

[4-BrPh(*n*Bu)Im]₂[Si(CN)₆] (6): 0.7 g (2.7 mmol) of potassium hexacyanidosilicate and 1.9 g (5.4 mmol, 2 equiv.) of [4-BrPh(*n*Bu)Im]Br was used. The product was crystallized from a mixture of acetonitrile and CH₂Cl₂ at -30 °C leading to formation of colorless crystals

in yields of 69 % (1.4 g, 1.8 mmol). $T_{\text{dec}} = 138$ °C. EA % calcd. (found) %: C 51.62 (51.18); H 4.33 (3.98); N 18.81 (18.34). (ESI)-MS (m/z) pos.: 279 ([4-BrPh(*n*Bu)Im]⁺); neg.: 106 ([Si(CN)₃]⁻); 158 ([Si(CN)₅]⁻). ¹H NMR (300 K, CD₃CN, 250.13 MHz): $\delta = 1.00$ (t, 6H, CH₂CH₃, ³J(¹H-¹H) = 7.3 Hz), 1.34–1.55 (m, 4H, CH₂CH₃), 1.95–2.05 (m, 4H, CH₂CH₂), 4.29 (t, 4H, NCH₂, ³J(¹H-¹H) = 7.4 Hz), 7.55–7.62 (m, 4H, *m*-CH), 7.62–7.68 (m, 2H, NCHCHN-*n*Bu), 7.76–7.82 (m, 4H, *o*-CH), 7.83–7.88 (m, 2H, NCHCHN-*n*Bu), 8.99–9.12 (m, 2H, NCHN). ¹³C{¹H} NMR (300 K, CD₃CN, 75.5 MHz): $\delta = 13.7$ (s, CH₂CH₃), 20.0 (s, CH₂CH₃), 32.4 (s, CH₂CH₂), 51.0 (s, NCH₂), 122.7 (s, NCHCHN-*n*Bu), 124.4 (s, NCHCHN-*n*Bu), 124.4 (s, *ipso*-C-Br), 125.4 (s, C_{Ar}yl), 134.3 (s, *ipso*-CN), 135.2 (s, C_{Ar}yl), 135.7 (s, NCHN), 140.0 (s, Si(CN)₆). ²⁹Si(IG) NMR (300 K, CD₃CN, 99.3 MHz) not observed (Si(CN)₆). IR (ATR, 298 K, 32 scans, cm⁻¹): $\tilde{\nu} = 422$ (w), 435 (w), 455 (w), 470 (w), 519 (s), 567 (vs), 633 (w), 647 (w), 703 (w), 750 (m), 789 (vw), 826 (m), 857 (w), 956 (w), 975 (vw), 1010 (w), 1045 (w), 1065 (m), 1100 (vw), 1121 (vw), 1131 (vw), 1195 (m), 1212 (w), 1255 (vw), 1282 (vw), 1294 (vw), 1319 (vw), 1331 (w), 1370 (w), 1389 (vw), 1412 (w), 1424 (w), 1436 (vw), 1459 (w), 1490 (m), 1548 (m), 1564 (w), 1607 (w), 1900 (vw), 2170 (vw), 2357 (vw), 2862 (w), 2928 (w), 2967 (w), 3077 (w), 3097 (w), 3142 (w), 3165 (vw). Raman (laser: 633 nm, accumulation time: 4 s, 25 scans, 298 K, cm⁻¹): $\tilde{\nu} = 78$ (5), 96 (7), 125 (6), 223 (1), 242 (1), 272 (0), 314 (1), 324 (1), 376 (1), 408 (1), 464 (2), 522 (1), 621 (1), 631 (1), 648 (1), 701 (1), 729 (2), 750 (1), 758 (1), 818 (1), 857 (1), 880 (1), 956 (4), 974 (1), 1011 (1), 1024 (1), 1065 (1), 1076 (2), 1099 (1), 1131 (1), 1185 (1), 1196 (1), 1254 (1), 1301 (1), 1330 (1), 1340 (1), 1349 (1), 1360 (4), 1388 (1), 1410 (1), 1425 (4), 1437 (2), 1457 (1), 1491 (1), 1550 (1), 1563 (1), 1591 (4), 2122 (1), 2162 (1), 2172 (10), 2862 (1), 2878 (1), 2899 (1), 2913 (1), 2919 (1), 2922 (1), 2929 (1), 2940 (1), 2964 (1), 3066 (1), 3076 (1), 3117 (1), 3141 (1), 3167 (1).

[Mes(*n*Bu)Im]₂{Si(CN)B(C₆F₅)₃]₆ (**8**): 0.07 g (0.10 mmol) of **3** is dissolved in 7 mL of dichloromethane. 0.37 g (0.73 mmol, 7 equiv.) of B(C₆F₅)₃ is dissolved in 8 mL of dichloromethane and added to the silicate solution with a syringe. Stirring the mixture at room temperature for one hour leads to formation of a white precipitate which is filtered off and washed three times with 5 mL of *n*-hexane to remove excess of B(C₆F₅)₃. Crystals of the dichloromethane hexasolvate [Mes(*n*Bu)Im]₂{Si(CN)B(C₆F₅)₃]₆·6CH₂Cl₂ (**7**) can be obtained by recrystallization from hot dichloromethane. Drying the crystals at 100 °C in vacuo leads to 0.30 g (0.08 mmol) of colorless and solvate-free product (**8**) in yields of 80 %. Note: Crystals of **7** can be obtained when combining a dichloromethane solution of both starting materials and placing the mixture at a vibration-free place. $T_{\text{dec}} = 230$ °C (**8**), $T_{\text{dec}} = 215$ °C (**7**). EA % calcd. (found) %: C 46.85 (47.15); H 1.24 (1.05); N 3.74 (3.79). (ESI)-MS (m/z) pos.: 243 ([Mes(*n*Bu)Im]⁺); neg.: *n.o.* ([anion]⁻)*; 528 ([[(HO)B(C₆F₅)₃]⁻]*); 543 ([[(MeO)B(C₆F₅)₃]⁻]*). ¹H NMR (300 K, CD₂Cl₂, 500.13 MHz): $\delta = 0.98$ (t, 6H, CH₂CH₃, ³J(¹H-¹H) = 7.2 Hz), 1.32–1.44 (m, 4H, CH₂CH₃), 1.91–1.98 (m, 4H, CH₂CH₂), 2.02 (s, 12H, *o*-CH₃), 2.35 (s, 6H, *p*-CH₃), 4.30 (t, 4H, NCH₂, ³J(¹H-¹H) = 7.3 Hz), 7.08 (s, 4H, *m*-CH), 7.34–7.36 (m, 2H, NCHCHN-*n*Bu), 7.52–7.54 (m, 2H, NCHCHN-*n*Bu), 8.18–8.20 (m, 2H, NCHN). ¹¹B{¹H} NMR (298 K, CD₂Cl₂, 160.5 MHz) -9.9 (br, $\Delta\nu_{1/2} = 1060$ Hz, B(C₆F₅)₃). ¹³C{¹H} NMR (298.1 K, CD₂Cl₂, 125.7 MHz): $\delta = 13.3$ (s, CH₂CH₃), 17.2 (s, *o*-CH₃), 19.7 (s, CH₂CH₃), 21.1 (s, *p*-CH₃), 32.2 (s, CH₂CH₂), 51.2 (s, NCH₂), 114.4–115.0 (m, *ipso*-CB); 123.1 (s, NCHCHN-*n*Bu), 124.9 (s, NCHCHN-*n*Bu) 129.2 (s, *ipso*-C_{para}), 130.0 (s, *m*-CH), 133.9 (s, *ipso*-C_{ortho}), 134.3 (s, NCHN), 135.6–138.2 (dm, *m*-CF); 138.9–141.4 (dm, *p*-CF); 142.5 (s, *ipso*-CN); 146.6–149.2 (o-CF); *n.o.* (Si(CN)₆). ¹⁹F{¹H} NMR (298 K, CD₂Cl₂, 470.5 MHz) -135.2 to -134.6 (m; *o*-CF), -158.6 to -158.1 (m, *p*-CF); -165.7 to -165.1 (m, *m*-CF). ²⁹Si(IG) NMR (300 K, CD₃CN, 99.3 MHz) not observed (Si(CN)₆).^[†] IR (ATR, 298 K, 32 scans, cm⁻¹): $\tilde{\nu} = 406$ (w), 445 (w), 470

(m), 488 (w), 501 (w), 556 (w), 575 (s), 587 (m), 616 (m), 631 (m), 686 (s), 729 (w), 742 (m), 771 (m), 797 (m), 843 (w), 863 (m), 874 (w), 973 (vs), 1012 (w), 1069 (w), 1102 (s), 1156 (vw), 1195 (w), 1286 (m), 1385 (m), 1457 (vs), 1519 (s), 1550 (vw), 1562 (vw), 1609 (vw), 1646 (m), 1710 (vw), 1743 (vw), 2271 (vw), 2322 (vw), 2361 (vw), 2374 (vw), 2413 (vw), 2559 (vw), 2576 (vw), 2582 (vw), 2644 (vw), 2749 (vw), 2868 (vw), 2914 (vw), 2938 (vw), 2967 (vw), 2978 (vw), 3101 (vw), 3153 (vw), 3165 (vw). Raman (laser: 633 nm, accumulation time: 10 s, 25 scans, 298 K, cm⁻¹): $\tilde{\nu} = 120$ (2), 143 (2), 155 (2), 162 (2), 181 (2), 241 (2), 285 (2), 307 (2), 333 (2), 348 (1), 353 (2), 395 (4), 426 (1), 447 (6), 455 (1), 473 (2), 481 (4), 485 (3), 509 (6), 535 (1), 553 (1), 571 (2), 580 (4), 585 (10), 615 (1), 624 (1), 658 (1), 682 (1), 688 (1), 706 (1), 730 (1), 746 (2), 777 (1), 807 (4), 821 (2), 864 (1), 881 (1), 891 (1), 969 (2), 1025 (1), 1050 (1), 1069 (1), 1104 (1), 1111 (1), 1118 (1), 1125 (1), 1139 (1), 1160 (1), 1235 (1), 1248 (1), 1285 (1), 1314 (1), 1331 (1), 1340 (1), 1362 (1), 1372 (1), 1388 (2), 1394 (2), 1410 (1), 1452 (1), 1458 (1), 1477 (1), 1485 (1), 1521 (1), 1548 (1), 1609 (1), 1647 (2), 2219 (1), 2268 (9), 2347 (1), 2532 (1), 2750 (1), 2867 (1), 2880 (2), 2938 (2), 2968 (2), 2983 (2), 3039 (1), 3149 (1), 3173 (1).

Annotation: *Anion could not be detected, due to too large m/z ratio. Peaks at 528 and 543 are products that occur during sample preparation with MeOH (column eluent). †Species were not detected since concentration of the salt in the solvent is too low.

Conflict of Interest

The authors declare no conflict of interest.

Acknowledgments

We thank the Deutsche Forschungsgemeinschaft (DFG SCHU 1170/9-2, STR526/20-2), especially the priority program SPP 1708 for financial support. Open access funding enabled and organized by Projekt DEAL.

Keywords: Cyanides · Ion pairs · Silicates · Structure elucidation · Synthetic methods

- [1] P. Walden, *Bull. l'Académie impériale des Sci. Saint-Petersbourg*. **1914**, *8*, 405–422.
- [2] P. Wasserscheid, T. Welton, *Ionic Liquids in Synthesis*, Wiley-VCH, Weinheim, **2008**.
- [3] P. Wasserscheid, W. Keim, *Angew. Chem. Int. Ed.* **2000**, *39*, 3772–3789; *Angew. Chem.* **2000**, *112*, 3926–3945.
- [4] H. Olivier-Bourbigou, L. Magna, D. Morvan, *Appl. Catal. A* **2010**, *373*, 1–56.
- [5] A. D. Sawant, D. G. Raut, N. B. Darvatkar, M. M. Salunkhe, *Green Chem. Lett. Rev.* **2011**, *4*, 41–54.
- [6] S. Seki, Y. Kobayashi, H. Miyashiro, Y. Ohno, A. Usami, Y. Mita, M. Watanabe, N. Terada, *Chem. Commun.* **2006**, 544–545.
- [7] I. Osada, H. de Vries, B. Scrosati, S. Passerini, *Angew. Chem. Int. Ed.* **2016**, *55*, 500–513; *Angew. Chem.* **2016**, *128*, 510.
- [8] M. C. Buzzeeo, R. G. Evans, R. G. Compton, *ChemPhysChem* **2004**, *5*, 1106–1120.
- [9] H. Shobukawa, H. Tokuda, S.-I. Tabata, M. Watanabe, *Electrochim. Acta* **2004**, *50*, 305–309.
- [10] G. P. S. Lau, J.-D. Décoppet, T. Moehl, S. M. Zakeeruddin, M. Grätzel, P. J. Dyson, *Sci. Rep.* **2016**, *5*, 18158.
- [11] F. Mazille, Z. Fei, D. Kuang, D. Zhao, S. M. Zakeeruddin, M. Grätzel, P. J. Dyson, *Inorg. Chem.* **2006**, *45*, 1585–1590.
- [12] J. Wu, Z. Lan, J. Lin, M. Huang, Y. Huang, L. Fan, G. Luo, *Chem. Rev.* **2015**, *115*, 2136–2173.
- [13] A. P. Abbott, G. Capper, D. L. Davies, R. K. Rasheed, P. Shikotra, *Inorg. Chem.* **2005**, *44*, 6497–6499.

- [14] L. Fischer, T. Falta, G. Koellensperger, A. Stojanovic, D. Kogelnig, M. Galanski, R. Krachler, B. K. Keppler, S. Hann, *Water Res.* **2011**, *45*, 4601–4614.
- [15] N. Hirayama, *Solvent Extr. Res. Dev. Jpn.* **2011**, *18*, 1–14.
- [16] L. Schmolke, S. Lerch, M. Bülow, M. Siebels, A. Schmitz, J. Thomas, G. Dehm, C. Held, T. Strassner, C. Janiak, *Nanoscale* **2019**, *11*, 4073–4082.
- [17] a) S. Wegner, C. Janiak, *Top. Curr. Chem.* **2017**, *375*, 65. b) L. Schmolke, S. Lerch, M. Bülow, M. Siebels, A. Schmitz, J. Thomas, G. Dehm, C. Held, T. Strassner, C. Janiak, *Nanoscale*, **2019**, *11*, 4073–4082.
- [18] M. Knies, M. Kaiser, A. Isaeva, U. Müller, T. Doert, M. Ruck, *Chem. Eur. J.* **2018**, *24*, 127–132.
- [19] S. Wolf, W. Klopfer, C. Feldmann, *Chem. Commun.* **2018**, *54*, 1217–1220.
- [20] M. Knies, M. Kaiser, M. Lê Anh, A. Efimova, T. Doert, M. Ruck, *Inorganics* **2019**, *7*, 45.
- [21] R. P. Swatloski, S. K. Spear, J. D. Holbrey, R. D. Rogers, *J. Am. Chem. Soc.* **2002**, *124*, 4974–4975.
- [22] K. R. Seddon, *Nat. Mater.* **2003**, *2*, 363–365.
- [23] M. Masse, K. Massonne, K. Halbritter, R. Noe, M. Bartsch, W. Siegel, V. Stegmann, M. Flores, O. Huttenloch, M. Becker, *WO03/062171A2*, **2003**.
- [24] J. S. Wilkes, J. A. Levisky, R. A. Wilson, C. L. Hussey, *Inorg. Chem.* **1982**, *21*, 1263–1264.
- [25] S. Ahrens, A. Peritz, T. Strassner, *Angew. Chem. Int. Ed.* **2009**, *48*, 7908–7910; *Angew. Chem.* **2009**, *121*, 8048.
- [26] M. Kaliner, A. Rupp, I. Krossing, T. Strassner, *Chem. Eur. J.* **2016**, *22*, 10044–10049.
- [27] S. Stolte, T. Schulz, C. W. Cho, J. Arning, T. Strassner, *ACS Sustainable Chem. Eng.* **2013**, *1*, 410–418.
- [28] J. Harloff, D. Michalik, S. Nier, A. Schulz, P. Stoer, A. Villinger, *Angew. Chem. Int. Ed.* **2019**, *58*, 5452–5456; *Angew. Chem.* **2019**, *131*, 5506.
- [29] Z. M. Smallwood, M. F. Davis, J. G. Hill, L. J. R. James, P. Portius, *Inorg. Chem.* **2019**, *58*, 4583–4591.
- [30] H. Jacobsen, H. Berke, S. Döring, G. Kehr, G. Erker, R. Fröhlich, O. Meyer, *Organometallics* **1999**, *18*, 1724–1735.
- [31] K. Spannhoff, R. Rojas, R. Fröhlich, G. Kehr, G. Erker, *Organometallics* **2011**, *30*, 2377–2384.
- [32] I. C. Vei, S. I. Pascu, M. L. H. Green, J. C. Green, R. E. Schilling, G. D. W. Anderson, L. H. Rees, *Dalton Trans.* **2003**, 2550–2557.
- [33] J. Zhou, S. J. Lancaster, D. A. Walker, S. Beck, M. Thornton-Pett, M. Bochmann, *J. Am. Chem. Soc.* **2001**, *123*, 223–237.
- [34] A. Bernsdorf, H. Brand, R. Hellmann, M. Köckerling, A. Schulz, A. Villinger, K. Voss, *J. Am. Chem. Soc.* **2009**, *131*, 8958–8970.
- [35] P. Pyykkö, M. Atsumi, *Chem. Eur. J.* **2009**, *15*, 12770–12779.
- [36] R. M. Bozorth, *J. Am. Chem. Soc.* **1922**, *44*, 317–323.
- [37] K. Bläsing, J. Bresien, R. Labbow, A. Schulz, A. Villinger, *Angew. Chem. Int. Ed.* **2018**, *57*, 9170–9175; *Angew. Chem.* **2018**, *130*, 9311.
- [38] G. R. Fulmer, A. J. M. Miller, N. H. Sherden, H. E. Gottlieb, A. Nudelman, B. M. Stoltz, J. E. Bercaw, K. I. Goldberg, *Organometallics* **2010**, *29*, 2176–2179.
- [39] G. M. Sheldrick, *Acta Crystallogr., Sect. A Found. Adv.* **2015**, *71*, 3–8.
- [40] G. M. Sheldrick, *Acta Crystallogr., Sect. C Struct. Chem.* **2015**, *71*, 3–8.
- [41] G. M. Sheldrick, *SADABS*, **2004**.
- [42] F. Schroeter, J. Soellner, T. Strassner, *Chem. Eur. J.* **2019**, *25*, 2527–2537.

Received: March 22, 2020